

# Vibrational behaviour of a realistic amorphous-silicon model

J. K. Christie<sup>\*,1</sup>, S. N. Taraskin, S. R. Elliott

*Department of Chemistry, University of Cambridge, Lensfield Road, Cambridge, CB2 1EW, UK*

---

## Abstract

The vibrational properties of a high-quality realistic model of amorphous silicon are examined. The longitudinal and transverse dynamical structure factors are calculated, and fitted to a damped harmonic oscillator (DHO) function. The width  $\Gamma$  of the best-fit DHO to the longitudinal dynamical structure factor scales approximately as  $k^2$  for wavevectors  $k \lesssim 0.55\text{\AA}^{-1}$ , which is above the Ioffe-Regel crossover frequency separating the propagating and diffusing regimes, occurring at  $k = 0.38 \pm 0.03\text{\AA}^{-1}$ . Using the DHO function as a fitting function for the transverse dynamical structure factor (without theoretical justification), gives a dependence of  $\Gamma \propto k^\alpha$  with  $\alpha \sim 2.5$  for wavevectors  $k \lesssim 0.7\text{\AA}^{-1}$ . There was no evidence for  $\Gamma \propto k^4$  behaviour for either polarization.

*Key words:* Amorphous silicon, Phonons

*PACS:* 63.50.+x

---

## 1 Introduction

The physics of the atomic vibrations present in amorphous materials has been the subject of much investigation, see e.g. (1; 2; 3). Advances in experimental techniques such as inelastic neutron scattering (INS) (4), inelastic X-ray scattering (IXS) (3), hyper-Raman scattering (5) and terahertz time-domain absorption spectroscopy (6) have allowed vibrations with frequencies of the order of one terahertz ( $1\text{ THz} \sim 4.1\text{ meV}/\hbar$ ) to be examined. Vibrations at

---

\* Corresponding author.

*Email address:* jchristi@ictp.it (J. K. Christie).

<sup>1</sup> Present address: The Abdus Salam International Centre for Theoretical Physics, Strada Costiera 11, 34014 Trieste, Italy

these frequencies are of particular interest, as these frequencies are comparable to those of the boson peak (an excess of vibrational modes as compared to the Debye elastic waves) (7) and of the Ioffe-Regel (IR) crossover between propagation and diffusion (2; 8; 9) observed in amorphous materials.

Vibrations in amorphous materials can be characterised by the spectral density. The spectral-density operator is  $\hat{\mathbf{A}}(\epsilon) = \delta(\epsilon - \hat{\mathbf{D}})$ , where  $\epsilon = \omega^2$  is the squared vibrational frequency, and  $\mathbf{D}$  is the dynamical matrix (10). In the plane-wave basis, the matrix elements of the spectral-density operator  $\hat{\mathbf{A}}_{\mathbf{k}\beta}(\epsilon) = \langle \mathbf{k}\beta | \hat{A} | \mathbf{k}\beta \rangle$ , where  $\mathbf{k}$  is the wavevector and  $\beta$  is the polarization of the plane wave, are proportional to the dynamical structure factor  $S_{\beta}(\mathbf{k}, \omega)$  (7), which, for the longitudinal polarization ( $\beta = L$ ), is the quantity measured by INS or IXS (3).

This proportionality is straightforward to see. Into the expression for  $\hat{\mathbf{A}}_{\mathbf{k}\beta}(\epsilon)$  above, the resolution of the identity in the basis of the eigenvectors  $\{|\mathbf{e}_i\rangle\}$  of the dynamical matrix  $\mathbf{D}$  is substituted to give:

$$\hat{\mathbf{A}}_{\mathbf{k}\beta}(\epsilon) = \sum_{ij} \langle \mathbf{k}\beta | \mathbf{e}_i \rangle \langle \mathbf{e}_i | \delta(\epsilon - \hat{\mathbf{D}}) | \mathbf{e}_j \rangle \langle \mathbf{e}_j | \mathbf{k}\beta \rangle, \quad (1)$$

where  $i$  and  $j$  are labels for the eigenvectors, which are normalized to unity,  $\langle \mathbf{e}_i | \mathbf{e}_j \rangle = \delta_{ij}$ . This expression is equal to

$$\hat{\mathbf{A}}_{\mathbf{k}\beta}(\epsilon) = \sum_i |\langle \mathbf{e}_i | \mathbf{k}\beta \rangle|^2 \delta(\epsilon - \epsilon_i), \quad (2)$$

where  $\epsilon_i$  is the energy of eigenmode  $i$ . Transforming equation 2 into frequency space, via  $\epsilon = \omega^2$ , gives

$$\hat{\mathbf{A}}_{\mathbf{k}\beta}(\omega) = \frac{1}{2\omega} \sum_i |\langle \mathbf{e}_i | \mathbf{k}\beta \rangle|^2 \delta(\omega - \omega_i), \quad (3)$$

where  $\omega_i$  is the vibrational frequency of eigenmode  $i$ . Equation 3 is valid for a plane wave of any polarization  $\beta$ . At high temperature, and in the single-excitation approximation, the dynamical structure factor for the longitudinal polarization,  $\beta = L$ , is defined as (11):

$$S_{\beta=L}(\mathbf{k}, \omega) = \frac{k_B T k^2}{m\omega^2} \sum_i |\langle \mathbf{e}_i | \mathbf{k}, \beta = L \rangle|^2 \delta(\omega - \omega_i), \quad (4)$$

where  $k_B$  is Boltzmann's constant,  $T$  is the temperature, and  $m$  is the atomic mass, and the Debye-Waller factor has been ignored (as in (7)). This is clearly

proportional to the spectral-density operator  $\hat{\mathbf{A}}_{\mathbf{k}\beta}(\omega)$  in equation 3, with polarization  $\beta = L$ . By defining a plane wave as

$$|\mathbf{k}\beta\rangle = \frac{1}{\sqrt{N}} \sum_j \mathbf{n}_{\mathbf{k}\beta} e^{-i\mathbf{k}\cdot\mathbf{r}_j}, \quad (5)$$

where  $N$  is the number of atoms,  $\mathbf{n}_{\mathbf{k}\beta}$  is the polarization vector of the plane wave, and  $\mathbf{r}_j$  is the position vector of atom  $j$ , and substituting this into equation 4, an expression for the dynamical structure factor for any polarization  $\beta$  can be derived as

$$S_\beta(\mathbf{k}, \omega) = \frac{k_B T k^2}{m\omega^2} \sum_i \left| \sum_j (\mathbf{n}_{\mathbf{k}\beta} \cdot \mathbf{e}_i^{(j)}) e^{-i\mathbf{k}\cdot\mathbf{r}_j} \right|^2 \delta(\omega - \omega_i), \quad (6)$$

where  $\mathbf{e}_i^{(j)}$  is the displacement vector of atom  $j$  vibrating in eigenmode  $i$ . The transverse dynamical structure factor  $S_T(\mathbf{k}, \omega)$  is not readily accessible in scattering experiments, but can easily be calculated from simulation. In practice, the orientationally averaged dynamical structure factor  $S_L(k, \omega)$  is obtained from scattering experiments (3), and, in this paper, both the orientationally averaged dynamical structure factors  $S_{L,T}(k, \omega)$  are calculated for *a*-Si.

As observed in experiment,  $S_L(k, \omega)$  of an amorphous material exhibits a single peak for low values of wavevector  $k$  (2; 3). The frequency at which this peak is located increases linearly with increasing  $k$  (at least for low  $k$ ); this is the regime of linear dispersion. The width of this peak also increases with increasing  $k$ , but more rapidly. Eventually, the width of the peak therefore becomes comparable to the peak frequency. The frequency at which this happens (typically  $\sim 1$  THz) is called the Ioffe-Regel (IR) crossover frequency (12). Above this frequency, the mean free path of the wave is shorter than the wavelength, and the external waves do not propagate in the conventional sense, instead transferring energy by diffusion (13).

These basic features are undisputed, but large uncertainties in the experimental data (see, e.g., (14)) have meant that it has been difficult to decide between the two main theoretical models for the behaviour of vibrational plane waves in amorphous materials. The first of these (3) suggests that the memory function is the sum of two processes: structural relaxation, assumed to be too slow to have an effect on vibrational timescales, and an instantaneous (or at least very fast) process, usually represented as a  $\delta$ -function in time (3). This leads to  $S_L(k, \omega)$  having the form of a damped harmonic oscillator (DHO) function (3). Fitting a DHO function to the experimentally observed peak gives a width  $\Gamma$  which scales roughly as the square of the wavevector,  $\Gamma \propto k^2$ , for many materials (3). This relationship is often seen to hold up to frequencies above the IR crossover. The second of these models (see, e.g., (15)) is based on an effective-

medium approximation (EMA) (16) and asserts that, in the region of the IR crossover, a DHO function is not a valid fit to  $S_L(k, \omega)$ , and that the scattering becomes much stronger (see, e.g., (15)). A functional form for  $S_L(k, \omega)$  is used which imposes  $\Gamma \propto k^4$  by construction, and this has given good fits of the dynamical structure factor at frequencies close to the IR crossover (14). The behaviour  $\Gamma \propto k^4$  was also found recently on fitting a DHO function to  $S_L(k, \omega)$  of lithium diborate glass (2). Recent inelastic ultra-violet scattering measurements (17) on vitreous silica suggest that there may be three regimes at different frequencies, with  $\Gamma \propto k^2$ ,  $\Gamma \propto k^4$  and  $\Gamma \propto k^2$  respectively.

The simplest possible model for the effect of disorder on vibrations, a force-constant-disordered lattice, gives  $\Gamma \propto k^4$  (18; 19). A theoretical model (20; 21) which includes positional disorder predicts  $\Gamma \propto k^2$ , but the model is one in which the dynamical matrix is assumed to be a Euclidean random matrix, and the positions of the atoms are taken to be uncorrelated and random. It is not clear how representative such a model is of real amorphous systems.

Further investigation of the behaviour of the width  $\Gamma(k)$  of  $S_L(k, \omega)$  might therefore be useful to decide on the generality or otherwise of these models. Investigating  $S_L(k, \omega)$  by simulation is helpful, because the large error bars which characterize the experimental results are absent. Simulated vitreous silica has been shown to have  $\Gamma \propto k^2$  (9; 22) using a DHO function, and fitting Lorentzian functions to  $S_L(k, \omega)$  of amorphous silicon (*a*-Si), simulated with the Stillinger-Weber potential (23), also resulted in a  $\Gamma \propto k^2$  dependence for  $k \lesssim 0.3 \text{ \AA}^{-1}$  (24). In this paper, we also examine the wavevector dependence of  $\Gamma$  in a simulated model of *a*-Si, but one simulated using the more physically realistic modified Stillinger-Weber potential (25), as described in the next section, as well as fitting to  $S_L(k, \omega)$  using the DHO fitting function. Fitting Lorentzian functions to  $S_T(k, \omega)$  of *a*-Si, produced behaviour suggestive of a  $\Gamma \propto k^2$  dependence for  $k \lesssim 0.3 \text{ \AA}^{-1}$  (26), but this model was also constructed with the Stillinger-Weber potential. The behaviour of both  $S_L(k, \omega)$  and  $S_T(k, \omega)$  is investigated here up to wavevectors of  $k \sim 2.0 \text{ \AA}^{-1}$ , which allows us to show where the DHO fitting function breaks down, and to investigate the vibrational properties of this model of *a*-Si at frequencies above the Ioffe-Regel crossover.

## 2 Methods

The model of *a*-Si studied here is a 4096-atom cubic model with box-size  $43.274 \text{ \AA}$  created by G. T. Barkema using a modified WWW method (27), and then relaxed by us (28) using the modified Stillinger-Weber (mSW) interatomic potential (25). The dynamical matrix was diagonalized using a Lanczos

routine (29). The dynamical structure factors were calculated using equation 6. To remove unimportant physical constants, the modified dynamical structure factor  $S_{\beta}^*(k, \omega) = \frac{m}{k_B T} S_{\beta}(k, \omega)$  is plotted here, where the polarization  $\beta = L$  or  $T$ , as in (11). These modified dynamical structure factors were fitted either to a single DHO function with two free parameters: peak frequency  $\Omega$  and width  $\Gamma$ , or to a sum of two DHO functions (for certain wavevectors) with five free parameters: peak frequencies and widths of the two DHO functions, and the ratio of their intensities. The peak normalization is fixed via  $\int \hat{\mathbf{A}}_{\mathbf{k}\beta}(\epsilon) d\epsilon = 1$ . To prevent artefacts, all data below  $\omega = 2.5$  meV were ignored in the fitting; the lowest non-zero vibrational frequency for this model is  $\omega \sim 3.7$  meV (at this frequency, the modes are of mostly transverse character, as seen by the peak in  $S_T(k, \omega)$  at this frequency in Figure 8). Due to the finite size of the model, the lowest value of wavevector  $k$  compatible with the periodic boundary conditions is  $k = 0.145 \text{\AA}^{-1}$ .

Strictly speaking, the dynamical structure factor is a weighted sum of delta-functions, with non-zero values only at frequencies equal to the mode frequencies (see equation 6). However, for ease of representation, the delta-functions in the spectral densities were broadened, before fitting, by a Lorentzian function with width  $\Gamma_{\text{br}}$ . The width  $\Gamma_{\text{br}}$  of the broadening chosen has a small, but noticeable, effect on the value of the width  $\Gamma$  of the best-fit DHO function, and hence on the value of the exponent  $\alpha$  in the expression  $\Gamma \propto k^{\alpha}$ .  $\Gamma_{\text{br}}$  was usually chosen to be larger than a few energy-level spacings (the mean energy-level spacing in this model is  $\sim 0.007$  meV), to smooth the data effectively for fitting. However, the larger  $\Gamma_{\text{br}}$  becomes, the greater is the effect on the raw data.

Increasing the value of  $\Gamma_{\text{br}}$  tends to decrease the value of  $\alpha$ . This is to be expected, if we assume that the effect of the Lorentzian broadening is to increase the true width by an amount comparable to  $\Gamma_{\text{br}}$ . If the true widths are plotted on a double-logarithmic plot, then adding a constant  $\Gamma_{\text{br}}$  to each width will shift the low- $\Gamma$  points further up the plot than the high- $\Gamma$  points. This will have the overall effect of reducing the gradient of the straight-line fitted to the broadened data. A value of  $\Gamma_{\text{br}}$  is required which provides a compromise between producing broadened data that are smooth enough to be fitted reliably, but giving small enough broadening so that the data are not greatly affected. For the longitudinal polarization, values of  $\Gamma_{\text{br}}$  in the range  $0.03 - 0.07$  meV were used (the narrowest peak has width  $\sim 0.2$  meV), and for the transverse polarization, values of  $\Gamma_{\text{br}}$  in the range  $0.015 - 0.04$  meV were used (the narrowest peak has width  $\sim 0.15$  meV).

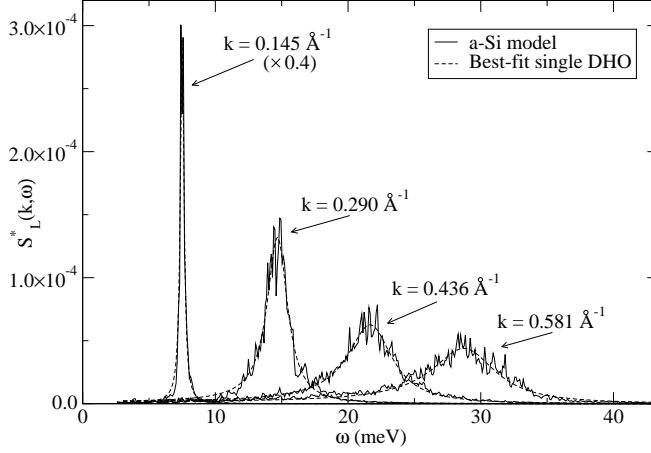


Fig. 1. The modified longitudinal dynamical structure factor  $S_L^*(k, \omega)$  of the realistic  $a$ -Si model, for values of wavevector  $k \lesssim 0.6 \text{ \AA}^{-1}$ , and the corresponding best-fit DHO functions. The width  $\Gamma_{\text{br}}$  of the broadening used was 0.05 meV.

### 3 Results

#### *Longitudinal polarization*

Figure 1 shows representative longitudinal modified dynamical structure factors  $S_L^*(k, \omega)$  for values of wavevector  $k \lesssim 0.6 \text{ \AA}^{-1}$ , together with their best-fit DHO functions. It is clear that, in this wavevector range,  $S_L^*(k, \omega)$  has only one peak, and that, for these wavevectors, the dynamical structure factor is well described by the DHO function. The DHO function sometimes deviates slightly from the data, e.g. on the low-energy side at around  $\omega \sim 10$  meV of the  $k = 0.290 \text{ \AA}^{-1}$  peak, but these deviations are small.

The width  $\Gamma$  of the best-fit DHO function is presented in Figure 2, as a function of wavevector  $k$ , on a double-logarithmic scale, for a representative value of  $\Gamma_{\text{br}} = 0.05$  meV. In Figure 2, the data points are seen to lie roughly on a straight line, indicating that a power-law dependence,  $\Gamma \propto k^\alpha$ , is an appropriate description. Other values of  $\Gamma_{\text{br}}$  give a width  $\Gamma$  which exhibits power-law behaviour as well. Figure 2 also shows the best-fit  $\Gamma \propto k^2$  ( $\alpha = 2$ ),  $\Gamma \propto k^4$  ( $\alpha = 4$ ), and unconstrained  $\alpha$  lines to the data in the range  $0.145 < k < 0.5 \text{ \AA}^{-1}$ . If  $\alpha$  is allowed to vary, then the best-fit value of  $\alpha$  for these data is  $2.24 \pm 0.07$  (this error is estimated by using the sum-of-squares deviation of the data from the best-fit straight line). The best-fit  $\Gamma \propto k^2$  line is shown to be close to the data, while  $\Gamma \propto k^4$  does not represent the data at all.

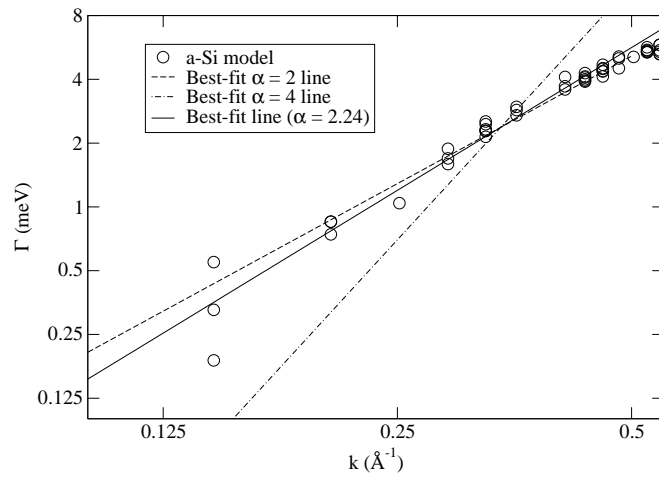


Fig. 2. The width  $\Gamma$  of the best-fit DHO function to the modified longitudinal dynamical structure factor  $S_L^*(k, \omega)$  of the realistic *a*-Si model with  $\Gamma_{\text{br}} = 0.05$  meV, on a double-logarithmic scale, with best-fit  $\alpha = 2$ ,  $\alpha = 4$ , and  $\alpha$ -unconstrained lines, where  $\Gamma \propto k^\alpha$ , fitted to the data in the range  $0.145 < k < 0.5 \text{\AA}^{-1}$ .

The precise value of  $\alpha$  obtained from data such as those in Figure 2 depends on the value of broadening  $\Gamma_{\text{br}}$  used, and the range of wavevectors studied. It will become clear from the next section (Figure 4) that the power-law behaviour  $\Gamma \propto k^\alpha$  is not obeyed for  $k \gtrsim 0.55 \text{\AA}^{-1}$ . Hence data sets were generated for values of broadening  $0.03 < \Gamma_{\text{br}} < 0.07 \text{ meV}$ , and ranges of wavevector starting at  $0.145 < k_{\text{min}} < 0.26 \text{\AA}^{-1}$  (to remove possible finite-size effects), and extending up to  $0.45 < k_{\text{max}} < 0.55 \text{\AA}^{-1}$ . For these data sets, the mean value of  $\alpha$  was 2.08, with a standard deviation of 0.15. 98% of the data sets had  $\alpha$  within  $\pm 0.3$  of this mean. For no value of broadening  $\Gamma_{\text{br}}$  or wavevector range was a line with  $\alpha = 4$  found to be close to the data.

The Ioffe-Regel (IR) crossover for this model of *a*-Si was estimated, defining it to occur at  $\Gamma \sim \Omega/2\pi$  (7), where  $\Omega$  is the excitation frequency in  $S_L^*(k, \omega)$ . For a given value of  $\Gamma_{\text{br}}$  and range of wavevector  $k$ , an estimate of the error in the IR crossover frequency was made, by using the sum-of-squares deviation from the best-fit straight-line (on a double-logarithmic plot) to obtain errors on the value of  $\alpha$ , and the sound velocity. As a first approximation, the IR crossover was assumed to lie in the centre of the overlap region of the two sets of error bars. Figure 3 displays this procedure for  $\Gamma_{\text{br}} = 0.05 \text{ meV}$  and wavevectors  $0.145 < k < 0.5 \text{\AA}^{-1}$ . The longitudinal IR crossover frequency was found to be  $\Omega_{\text{IR},L} = 19.1 \pm 1.3 \text{ meV}$ , corresponding to a wavevector of  $k_{\text{IR},L} = 0.38 \pm 0.03 \text{\AA}^{-1}$ . This is somewhat lower than the previous estimate of  $\sim 25 \text{ meV}$  (24), due, presumably, to the different interatomic potential and fitting function used here. Different values of  $\Gamma_{\text{br}}$  and wavevector range give values of  $\Omega_{\text{IR},L}$  within the error bars given above.

It follows from this value of  $\Omega_{\text{IR},L}$  and Figure 3 that the approximate  $\Gamma \propto k^2$  behaviour for longitudinal modes for this model of *a*-Si continues to frequencies and wavevectors above the IR crossover frequency and wavevector, as found in experiment and simulations for other materials (3), if the DHO fitting function is used. There is no sharp change in the behaviour of  $S_L^*(k, \omega)$  evident at or around the IR crossover frequency for this model (Figure 1), nor in the pseudo-dispersion law  $\Omega = c_L k$ , with  $c_L \sim 7670 \text{ m s}^{-1}$  (Figure 3).

At higher wavevectors, the DHO fitting function ceases to produce a good fit (Figure 5). In addition, for wavevectors in the range  $0.55 < k < 0.8 \text{\AA}^{-1}$ , the peak in  $S_L^*(k, \omega)$  narrows (Figure 4), although the excitation frequency continues to increase monotonically (Figure 5). This narrowing is thought to be related to remnants of vibrational-mode localization occurring in the gap in the vibrational density of states between the acoustic and optic bands, at  $\omega \sim 35 \text{ meV}$ . (Peak excitation frequencies for  $0.55 < k < 0.8 \text{\AA}^{-1}$  occur in this region.) This is shown in Figure 6, where the inverse participation ratio of an eigenmode, defined as  $(\sum_i e_i^2)^2 / N \sum_i e_i^4$ , where  $e_i$  is the amplitude of the displacement of atom  $i$  in that mode, and  $N$  is the number of atoms, is shown



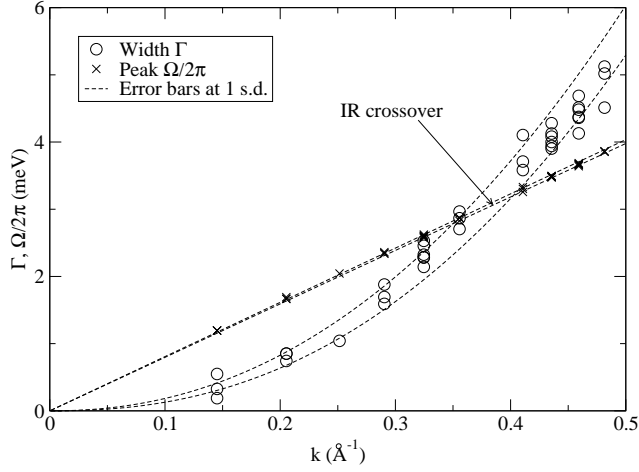


Fig. 3. The width  $\Gamma$  of the best-fit DHO to the modified longitudinal dynamical structure factor  $S_L^*(k, \omega)$  of the realistic  $a$ -Si model, with broadening  $\Gamma_{\text{br}} = 0.05$  meV, and the scaled peak frequency  $\Omega/2\pi$ , plotted against wavevector  $k$ , with errors to the best-fit lines. The IR crossover occurs in the region where the error bars overlap.

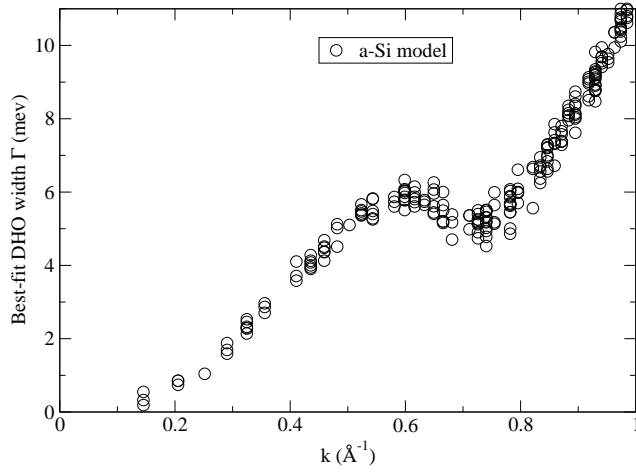


Fig. 4. The width  $\Gamma$  of the best-fit DHO to the modified longitudinal dynamical structure factor  $S_L^*(k, \omega)$  of the realistic  $a$ -Si model with  $\Gamma_{\text{br}} = 0.05$  meV.

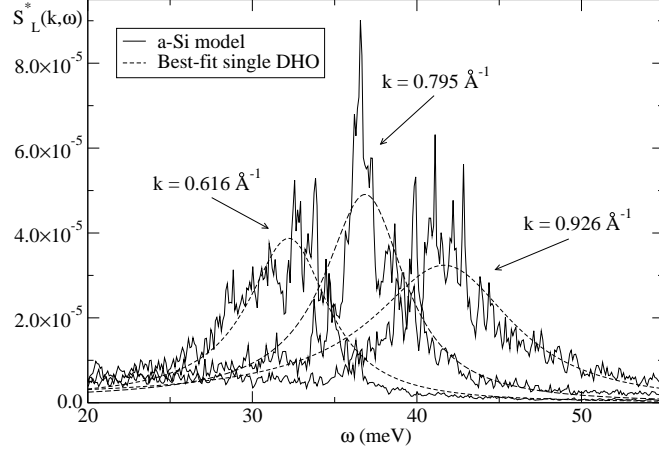


Fig. 5. The modified longitudinal dynamical structure factor  $S_L^*(k, \omega)$  of the realistic  $a$ -Si model, for values of wavevector  $0.6 \lesssim k \lesssim 1.0 \text{ \AA}^{-1}$ , and the best-fit DHO functions. The width of the broadening used was  $\Gamma_{\text{br}} = 0.05 \text{ meV}$ .

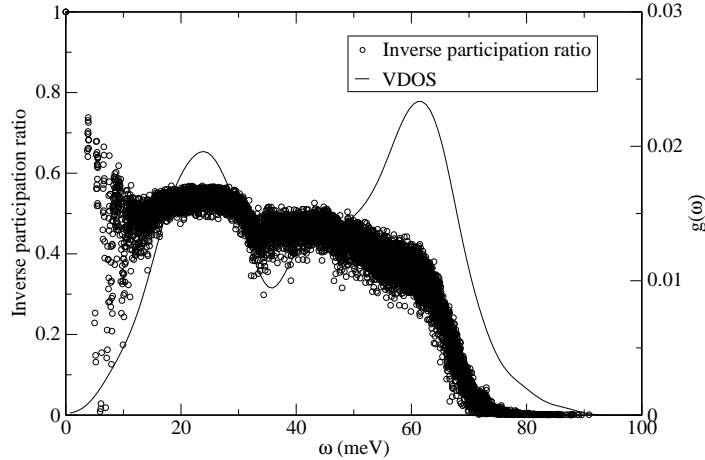


Fig. 6. The inverse participation ratio and vibrational density of states  $g(\omega)$  of the realistic  $a$ -Si model.

and is seen to decrease (indicating greater localization) at roughly the same frequency ( $\omega \sim 35$  meV) as the dip in the vibrational density of states between the overlapping bands. This anomalous dip in  $\Gamma(k)$  (Figure 4) at  $k \sim 0.7\text{\AA}^{-1}$  is not associated with the IR crossover, which occurs at  $k_{IR,L} \sim 0.38\text{\AA}^{-1}$  (Figure 5).

At even higher wavevectors,  $k > 1.0\text{\AA}^{-1}$ , a second peak is evident in  $S_L^*(k, \omega)$  at low frequency (Figure 7). This peak is not accounted for either in the memory-function or EMA approaches, but in other materials is thought to be a signature of modes with a largely transverse character mixing with the longitudinal spectrum, this disorder-induced mode mixing being a result of the absence of purely polarized modes in an amorphous material, see, e.g., (3; 19). It will be clear from Figure 11 in the next section that the dominant peak in  $S_T^*(k, \omega)$  at high  $k$  indeed is responsible for the additional low-frequency peak in  $S_L^*(k, \omega)$ . For sufficiently large values of wavevector  $k$ , the spectral density becomes similar to the VDOS (7).

Figure 7 also shows the best-fit sum of two DHO functions, which give reasonable fits to the data. No quantitative analysis of the widths was performed for these wavevectors, as the memory-function approach does not predict the existence of this second peak, and so fitting the data to two DHO functions is largely done *ad hoc*. Also, for wavevectors  $1.0 \lesssim k \lesssim 1.3\text{\AA}^{-1}$  the second peak is small and flat. The widths found for this peak at these wavevectors vary significantly even for data from the same or very similar wavevectors, because the second-peak intensity is so small that its width can vary substantially without greatly affecting the sum-of-squares deviation. It is thus difficult to extract meaningful data about the peak widths for these wavevectors.

### *Transverse polarization*

Figure 8 shows representative transverse modified dynamical structure factors  $S_T^*(k, \omega)$ , and their best-fit DHO functions, for wavevectors  $k \lesssim 1.0\text{\AA}^{-1}$ . The width  $\Gamma_{\text{br}}$  of the broadening used was 0.02 meV. There is only one peak in  $S_T^*(k, \omega)$  at these frequencies. The memory-function approach does not predict a particular functional form for the peak shape in the transverse spectral density, nor in fact does any current theory (30). Therefore, different functional forms for the fitting function were tried in an *ad hoc* fashion: Gaussian, Lorentzian and DHO. At very low wavevectors,  $k \lesssim 0.4\text{\AA}^{-1}$ , the DHO and Lorentzian functions both gave good fits to the data. Above this wavevector, the DHO gave quantitatively the better fit to the data (in terms of having a lower sum-of-squares deviation), and this remained so for all wavevectors for which the data could reasonably be described by a single peak ( $k \lesssim 1.0\text{\AA}^{-1}$ ). For this reason, and to facilitate a comparison with the data for the longitudinal polarization, only the results from the DHO fitting function are considered

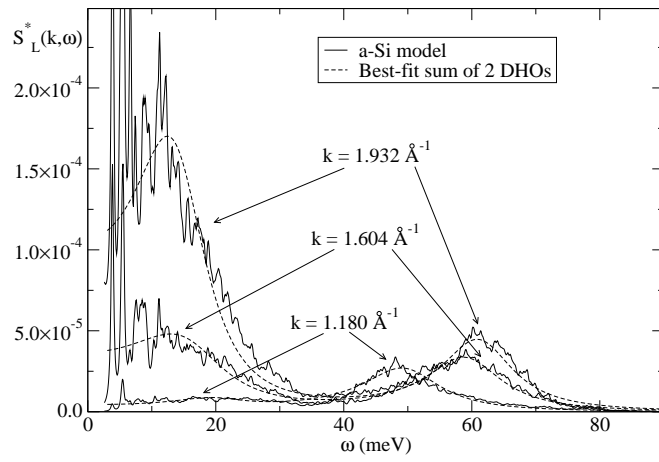


Fig. 7. The modified longitudinal dynamical structure factor  $S_L^*(k, \omega)$  of the realistic  $a$ -Si model, for values of wavevector  $k \gtrsim 1.0 \text{ \AA}^{-1}$ , and the best-fit sum of two DHO functions. The value of broadening used was  $\Gamma_{\text{br}} = 0.2 \text{ meV}$ .

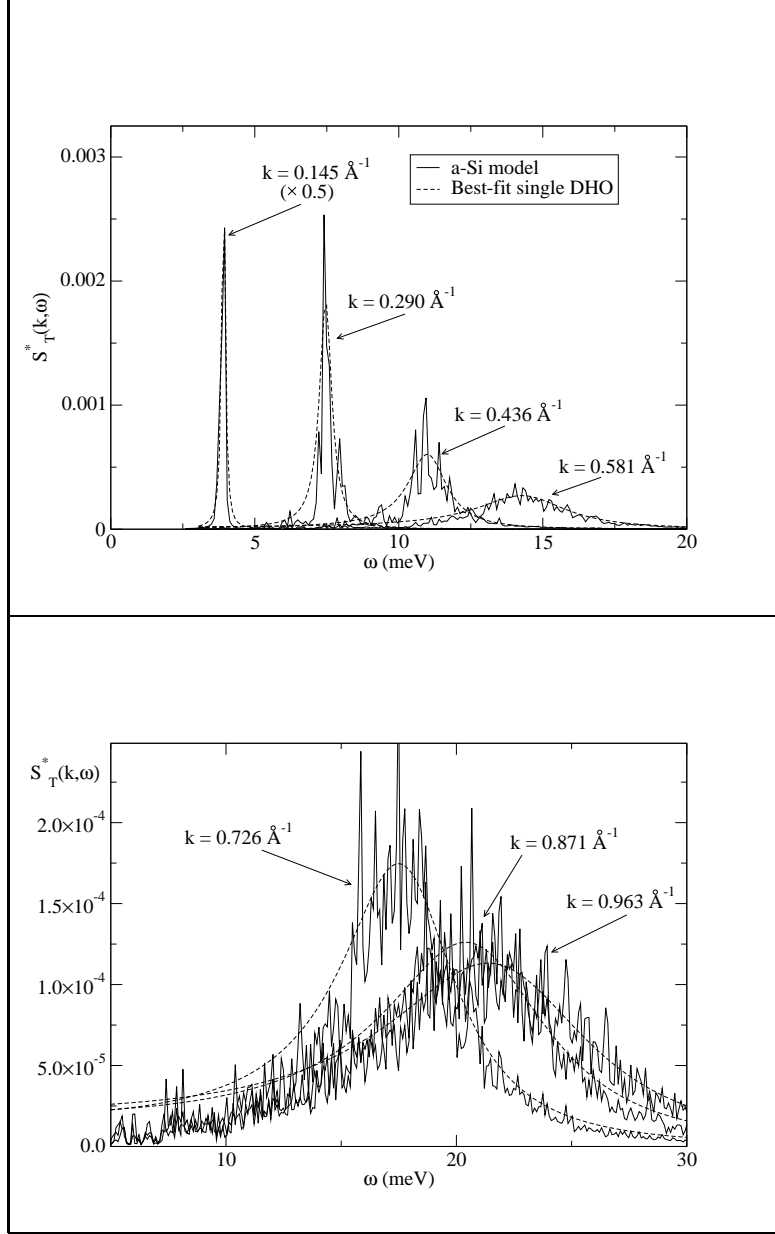


Fig. 8. The modified transverse dynamical structure factor  $S_T^*(k, \omega)$  of the realistic  $a$ -Si model, for values of wavevector  $k \lesssim 1.0 \text{ \AA}^{-1}$ , with the corresponding best-fit single DHO functions. The value of broadening used was  $\Gamma_{\text{br}} = 0.02 \text{ meV}$ .

here. From Figure 8, it is clear that the DHO function provides only a reasonable approximation to the data at low wavevectors. The noise in the data is due in part to the sparseness of eigenvalues at low frequencies.

As for the longitudinal case, the precise value of the exponent  $\alpha$  in the dependence  $\Gamma \propto k^\alpha$  depends on the value of broadening  $\Gamma_{\text{br}}$  used, and the range of wavevectors studied. For the transverse polarization, the physical relevance of the DHO best-fit width  $\Gamma$  is less clear, as there is no theoretical reason to expect the DHO function to be a good fit to  $S_T^*(k, \omega)$ . A discussion of such a

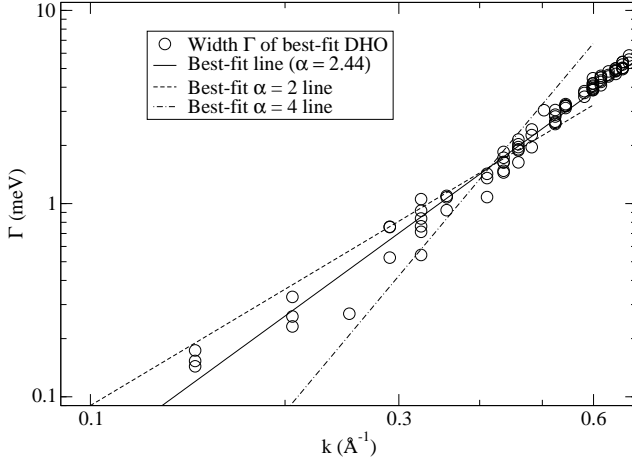


Fig. 9. The width  $\Gamma$  of the best-fit DHO to the modified transverse dynamical structure factor  $S_T^*(k, \omega)$  of the realistic  $\alpha$ -Si model, on a double-logarithmic scale, with best-fit  $\alpha = 2$ ,  $\alpha = 4$  and unconstrained- $\alpha$  straight lines fitted to the range  $0.145 < k < 0.6 \text{ \AA}^{-1}$ . The value of broadening used was  $\Gamma_{\text{br}} = 0.02 \text{ meV}$ .

fit is included here for completeness. Figure 9 shows the width  $\Gamma$  of the best-fit DHO functions to  $S_T^*(k, \omega)$  as a function of wavevector  $k$ , as well as the best-fit lines with  $\alpha = 2$ ,  $\alpha = 4$  and unconstrained  $\alpha$ , fitted to the wavevector range  $0.145 < k < 0.6 \text{ \AA}^{-1}$ , and with  $\Gamma_{\text{br}} = 0.02 \text{ meV}$ . Above  $k \sim 0.6 \text{ \AA}^{-1}$ , the DHO function gives a less good fit (Figure 8), and deviations from linear dispersion are also present. The value of  $\alpha$  in this case is  $2.44 \pm 0.05$ . It is clear that neither  $\alpha = 2$  or  $\alpha = 4$  represents the data well, although  $\alpha = 2$  is closer. The precise value of  $\alpha$  is likely to be strongly dependent on the fitting function used. For values of broadening  $0.015 < \Gamma_{\text{br}} < 0.04 \text{ meV}$  and for ranges of wavevector starting at  $0.145 < k_{\text{min}} < 0.26 \text{ \AA}^{-1}$ , and extending to  $0.5 < k_{\text{max}} < 0.7 \text{ \AA}^{-1}$ , the mean value of  $\alpha$  found was 2.54, with a standard deviation of 0.14. 96% of the data sets generated had  $\alpha$  within 0.3 of this mean. For no value of broadening or wavevector range did the exponent  $\alpha = 4$  give a good representation of the data.

Using the best-fit line for  $0.145 < k < 0.6 \text{ \AA}^{-1}$ , the transverse IR crossover was estimated to be at a frequency of  $\Omega_{IR,T} = 11.1 \pm 0.5 \text{ meV}$ , corresponding to a wavevector of  $k_{IR,T} = 0.44 \pm 0.02 \text{ \AA}^{-1}$  (Figure 10), using the same method as for the longitudinal polarization. This is lower than the previous estimate of  $\sim 17 \text{ meV}$  (24), but the different interatomic potential and fitting function used in this study may explain this. As for the longitudinal polarization, no sharp change is evident in the width or the shape of  $S_T^*(k, \omega)$  at the transverse IR crossover (Figure 8), nor in the pseudo-dispersion law  $\Omega = c_T k$ , with  $c_T \sim 3820 \text{ m s}^{-1}$  (Figure 10).

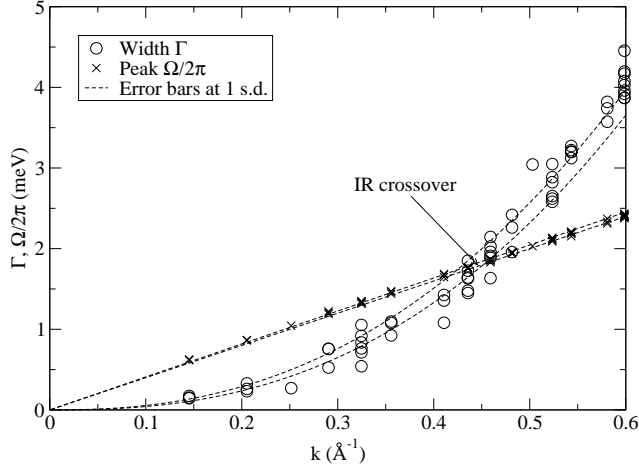


Fig. 10. The width  $\Gamma$  of the best-fit DHO to the modified transverse dynamical structure factor  $S_T^*(k, \omega)$  of the realistic  $a$ -Si model, with broadening  $\Gamma_{\text{br}} = 0.02$  meV, and the scaled peak frequency  $\Omega/2\pi$ , plotted against wavevector  $k$ , with errors to the best-fit lines. The IR crossover occurs in the region where the error bars overlap.

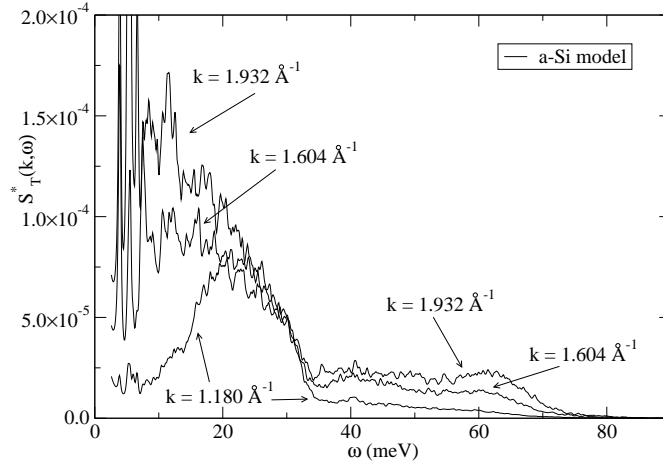


Fig. 11. The modified transverse dynamical structure factor  $S_T^*(k, \omega)$  of the realistic  $a$ -Si model, for values of wavevector  $k \gtrsim 1.0 \text{ \AA}^{-1}$ . The value of broadening used was  $\Gamma_{\text{br}} = 0.2$  meV.

For wavevectors above  $k \sim 1.0 \text{\AA}^{-1}$ ,  $S_T^*(k, \omega)$  has one dominant peak at low frequency, with a flat shoulder at higher frequencies (Figure 11). It is clear that a single peak fit is no longer an adequate description of the transverse dynamical structure factor in this wavevector region. Neither single DHO nor double DHO fits are very representative of the data for these wavevectors. As mentioned previously, the dominant low-frequency peak in  $S_T^*(k, \omega)$  appears in the longitudinal spectrum at high  $k$  (Figures 7,11), and, vice versa, the high-frequency peak in  $S_L^*(k, \omega)$  also begins to appear in the transverse spectra, indicative of strong mode mixing at such high values of  $k$ .

## 4 Discussion

The width  $\Gamma$  of the dynamical structure factor of amorphous materials increases with increasing wavevector  $k$ , but there is much dispute about the functional form of this increase. Broadly speaking, using a DHO fitting function (as proposed in (3)) to fit to the dynamical structure factor peaks gives a behaviour of  $\Gamma \propto k^2$  at low  $k$ , with the exception of lithium diborate, for which  $\Gamma \propto k^4$  (2) is found. A second method, based on an EMA approach (16), which involves modelling the dynamical structure factor with a function which has  $\Gamma \propto k^4$  by construction, has also yielded good fits at frequencies close to the Ioffe-Regel crossover between propagating and diffusive modes.

This paper describes a model of amorphous silicon which is shown to exhibit an approximate  $\Gamma \propto k^2$  dependence for the longitudinal dynamical structure factor. This relationship holds for peak frequencies above the IR crossover frequency, as has been found for other materials modelled with the DHO function (3). An *ad hoc* fitting of the transverse dynamical structure factor to a DHO function (without theoretical justification) gives a slightly higher exponent, about 2.5. For neither polarization was any evidence for  $\Gamma \propto k^4$  found, nor was there any sharp change in the behaviour of the dynamical structure factor at the IR crossover, as proposed in the EMA method.

The nature of vibrations in amorphous systems in this frequency region is not yet fully understood. It is known that a force-constant-disordered crystalline lattice gives  $\Gamma \propto k^4$  (18; 19), while many positionally disordered materials, including *a*-Si, give  $\Gamma \propto k^2$ , as does a positionally disordered analytical model (20; 21). It may therefore be positional disorder which is responsible for the reduction in the exponent from 4 to 2, although the mechanism of this reduction remains unclear. Of particular interest is the recent experimental work of Masciovecchio *et al.* (17), which suggests that there may be three regimes in vitreous silica, with respectively  $\Gamma \propto k^2$ ,  $\Gamma \propto k^4$  and  $\Gamma \propto k^2$ . If this behaviour is generally true, then these regions could occur at different ranges of wavevector for different materials, and this could account for different depen-



dences being observed between different materials, e.g. the  $\Gamma \propto k^4$  dependence in lithium diborate (2), and for the intermediate value of exponent  $\alpha = 2.54$  found for the transverse polarization above.

## 5 Acknowledgements

We thank G. T. Barkema for providing the coordinates of the model. J. K. C. is grateful to the Engineering and Physical Sciences Research Council for the provision of a Ph.D. studentship.

## References

- [1] S. R. Elliott, *Physics of Amorphous Materials*, 2nd edn., Longman (1990)
- [2] B. Rufflé, G. Guimbretière, E. Courtens, R. Vacher and G. Monaco, *Phys. Rev. Lett.* **96**, 045502 (2006)
- [3] G. Ruocco and F. Sette, *J. Phys.: Condens. Mat.* **13**, 9141 (2001)
- [4] E. Fabiani, A. Fontana and U. Buchenau, cond-mat/0502207 (2005)
- [5] G. Simon, B. Hehlen, E. Courtens, E. Longueteau and R. Vacher, *Phys. Rev. Lett.* **96**, 105502 (2006)
- [6] S. N. Taraskin, S. I. Simdyankin, S. R. Elliott, J. R. Neilson and T. Lo, *Phys. Rev. Lett.* **97**, 055504 (2006)
- [7] S. N. Taraskin and S. R. Elliott, *Europhys. Lett.* **39**, 37 (1997)
- [8] S. N. Taraskin and S. R. Elliott, *Phys. Rev. B* **61**, 12017 (2000)
- [9] S. N. Taraskin and S. R. Elliott, *Phys. Rev. B* **61**, 12031 (2000)
- [10] H. Ehrenreich and L. Schwartz, *Solid State Phys.* **31**, 149 (1976)
- [11] G. Ruocco, F. Sette, R. Di Leonardo, G. Monaco, M. Sampoli, T. Scopigno and G. Vilianni, *Phys. Rev. Lett.* **84**, 5788 (2000)
- [12] A. F. Ioffe and A. R. Regel, *Prog. Semicond.* **4**, 237 (1960)
- [13] P. B. Allen, J. L. Feldman, J. Fabian and F. Wooten, *Philos. Mag. B* **79**, 1715 (1999)
- [14] E. Courtens, M. Foret, B. Hehlen and R. Vacher, *Solid State Comm.* **117**, 185 (2001)
- [15] E. Rat, M. Foret, E. Courtens, R. Vacher and M. Arai, *Phys. Rev. Lett.* **83**, 1355 (1999)
- [16] G. Polatsek and O. Entin-Wohlman, *Phys. Rev. B* **37**, 7726 (1988)
- [17] C. Masciovecchio, G. Baldi, S. Caponi, L. Comez, S. Di Fonzo, D. Fioretto, A. Fontana, A. Gessini, S. C. Santucci, F. Sette, G. Vilianni, P. Vilmercati and G. Ruocco, *Phys. Rev. Lett.* **97**, 035501 (2006)
- [18] W. Schirmacher, G. Diezemann and C. Ganter, *Phys. Rev. Lett.* **81**, 136 (1998)

- [19] S. N. Taraskin, Y. L. Loh, G. Natarajan and S. R. Elliott, Phys. Rev. Lett. **86**, 1255 (2001)
- [20] V. Martin-Mayor, M. Mézard, G. Parisi and P. Verrocchio, J. Chem. Phys. **114**, 8068 (2001)
- [21] S. Ciliberti, T. S. Grigera, V. Martin-Mayor, G. Parisi and P. Verrocchio, J. Chem. Phys. **119**, 8577 (2003)
- [22] O. Pilla, S. Caponi, A. Fontana, J. R. Gonçalves, M. Montagna, E. Rossi, G. Vilianni, L. Angelani, G. Ruocco, G. Monaco and F. Sette, J. Phys.: Condens. Mat. **16**, 8519 (2004)
- [23] F. Stillinger and T. A. Weber, Phys. Rev. B **31**, 5262 (1985)
- [24] J. L. Feldman, J. Non-Cryst. Solids **307-310**, 128 (2002)
- [25] R. L. C. Vink, G. T. Barkema, N. Mousseau and W. F. van der Weg, J. Non-Cryst. Sol. **282**, 248 (2001)
- [26] J. L. Feldman, P. B. Allen and S. R. Bickham, Phys. Rev. B **59**, 3551 (1999)
- [27] G. T. Barkema and N. Mousseau, Phys. Rev. B **62**, 4985 (2000)
- [28] J. K. Christie, Ph.D. thesis, University of Cambridge, 2006
- [29] J. K. Cullum and R. A. Willoughby, *Lanczos Algorithms for Large Symmetric Eigenvalues Computations, Vol. 1, Theory*, Birkhauser, 1985
- [30] E. Pontecorvo, M. Krisch, A. Cunsolo, G. Monaco, A. Mermet, R. Verbeni, F. Sette and G. Ruocco, Phys. Rev. E **71**, 011501 (2005)